



**HAL**  
open science

## Parametric Study of Radio Propagation in Railways Based on Ray-Tracing Simulations

Jorge Elizalde, Aitor Arriola, Marti Roset, Jérôme Härri, Igor López, Marvin  
Straub

► **To cite this version:**

Jorge Elizalde, Aitor Arriola, Marti Roset, Jérôme Härri, Igor López, et al.. Parametric Study of Radio Propagation in Railways Based on Ray-Tracing Simulations. 2023 17th European Conference on Antennas and Propagation (EuCAP), Mar 2023, Florence, Italy. pp.1-5, 10.23919/EuCAP57121.2023.10133721 . hal-04135063

**HAL Id: hal-04135063**

**<https://hal.science/hal-04135063>**

Submitted on 20 Jun 2023

**HAL** is a multi-disciplinary open access archive for the deposit and dissemination of scientific research documents, whether they are published or not. The documents may come from teaching and research institutions in France or abroad, or from public or private research centers.

L'archive ouverte pluridisciplinaire **HAL**, est destinée au dépôt et à la diffusion de documents scientifiques de niveau recherche, publiés ou non, émanant des établissements d'enseignement et de recherche français ou étrangers, des laboratoires publics ou privés.

# Parametric Study of Radio Propagation in Railways Based on Ray-Tracing Simulations

Jorge Elizalde<sup>1,2</sup>, Aitor Arriola<sup>1,2</sup>, Marti Roset<sup>3</sup>, Jérôme Härrri<sup>4</sup>, Igor López<sup>5</sup>, Marvin Straub<sup>6</sup>

<sup>1</sup>HW and Communication Systems, IKERLAN Technology Research Centre, Arrasate, Spain, {jelizalde, aarriola}@ikerlan.es

<sup>2</sup>Basque Research and Technology Alliance (BRTA), Mendaro, Spain

<sup>3</sup>Systems Innovation, COMSA Corporación, Madrid, Spain, marti.rosset@comsa.com

<sup>4</sup>Communication System Department, EURECOM, Sophia-Antipolis, France, jerome.haerri@eurecom.fr

<sup>5</sup>Technology Division, CAF R&D, Beasain, Spain, igor.lopez@caf.net

<sup>6</sup>IP-TCN Communication, ALSTOM, Mannheim, Germany, marvin.straub@alstomgroup.com

**Abstract**—In this work the RF propagation has been characterized first for a 5G Wireless Train Backbone, based on a parametric simulation model of a train. Different parameters have been changed to study their effect on the RF propagation. According to these results, some recommendations are made. The antenna propagation has also been studied in a model for the Wireless Consist Network.

**Index Terms**— antennas, propagation, simulation, 5G, railway, WLTB, WLCN, Safe4RAIL-3

## I. INTRODUCTION

The wired Train Control and Monitoring System (TCMS) of the train has its wireless counterpart in the Wireless Train Backbone (WLTB) for inter-consist communications, and the Wireless Consist Network (WLCN) for intra-consist communications. It should be noted that a consist is formed by a group of train cars including the traction units. In these applications the environment is mostly metallic, so the transmission of the signal is going to be highly affected by these metallic parts, leading to a high amount of reflected and refracted paths that interact between them. Therefore, the simulation of the propagation of the signal can help engineers improve the communication.

Previous works have been focused on wireless communications between a train and ground-based antennas, in open air [1] and tunnels [2], or between trains [3], or between train cars with antennas located inside [4]. This paper extends the work described in [5], where simulations were presented for the WLTB. The location of the antennas was modified, and the impact of a tunnel and its material properties was analyzed for a WLTB at 5.9 GHz.

This previous work has been extended to study more variations of the train model configuration. It also covers simulations related to the internal communications inside a train car (WLCN). These simulations have been performed in three different scenarios.

The paper is structured as follows. The simulation models are detailed in Section II, which are simplified versions of a real train. In Section III the simulation results are presented for different roof configurations in the case of

WLTB, and for three different scenarios in the case of WLCN. Finally, conclusions and future work are presented in Section IV

## II. SIMULATION MODEL

In our models 2.45 GHz (Industrial, Scientific and Medical, ISM band), and 5.9 GHz (Safety Band reserved for transportation-related communications) frequencies have been selected for WLCN and WLTB respectively, and the models have the following maximum sizes, which are larger than  $10\lambda$ :

- Length: 30.5 m
- Width: 5.2 m
- Height: 5.0 m

To simulate the WLTB and WLCN, the SBR+ solver of ANSYS HFSS has been used. Both models have been built based on their respective CAD files of actual trains.

Simulations have been done extending the SBR method, based on the Physical Optics (PO), using Physical Theory of Diffraction (PTD), Uniform Theory of Diffraction (UTD), and enabling Creeping Wave (CW) physics. First, to limit the processing time, the ray density and number of bounces have been optimized for this model.

### A. Wireless Train Backbone

Concerning the train roof, multiple configurations are being implemented in the railway market: length, width, auxiliary boxes (number, location, and size), fairings or pantographs. Regarding the environment, there are also several elements that can modify the communication path between antennas: tunnels, track curve, viaducts, train stations, catenary systems, or masts. Therefore, a simulation model as generic as possible has been built to consider all these variations, and it has been parameterized to study the effect of each parameter. The simulation model has the following main features:

1. It is based on two train cars, one of them being the locomotive with a pantograph.

2. Train cars can be fitted with several boxes on the roof for auxiliary equipment.
3. Train cars can be fitted with fairings to protect the equipment on the roof and for improved aerodynamic behavior.
4. The model can be simulated inside a tunnel.
5. Train cars and tunnel can be bent according to the track curve radius.
6. Antennas can be tailored: type and radiation pattern.

The model is based on a *Compañía Auxiliar de Ferrocarriles S.A.* (CAF) commuter train. After importing the CAD model, it has been simplified using surfaces to emulate the external contour of the real train. The final model is shown in Fig. 1. The consist is composed of a train tractor unit with a pantograph, and a train car. On the roof of the train cars there are several metallic boxes in grey to accommodate different items, as the power converters or the air conditioning system. The model of the train is composed of metallic surfaces. A Perfect Electric Conductor (PEC) boundary has been established for these metallic surfaces.

Quarter-wave monopole antennas at 5.9 GHz have been used in the model, to emulate the omnidirectional radiation pattern of most railway antennas. The antennas are placed in the middle of the width of the train car. As initial positions for the antennas, the locations used for the Train-to-Ground (T2G) antennas have been taken, as they may allow a future combination of the T2G and WLTB links using the same antenna.

### B. Wireless Consist Network

The CAD model for the wireless link inside the consist is based on one of the train cars of *Deutsche Bahn's Advanced Train Lab*<sup>1</sup>. In this train car model, half-wave dipole antennas at 2.45 GHz have been used. The access point is located at the middle of the width of the train car, in the ceiling. Three scenarios have been analyzed:

1. *Sensors*: multiple devices located on the ceiling in any point of the train car.
2. *Surveillance cameras*: several devices in specific positions on the ceiling.
3. *Operator*: several devices in any point of the train car.

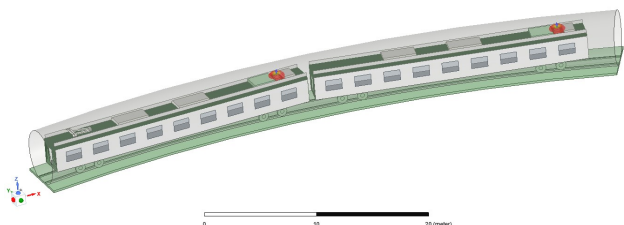


Fig. 1 Train model for WLTB

<sup>1</sup> <https://www.deutschebahn.com/en/Digitalization/The-fastest-lab-on-rails-6935126>

The train car model is showed in Fig. 2. Passengers are modelled as blue cylinders, and the operator as the yellow cylinder, all of them with relative permittivity and conductivity properties of human muscle at 2.45 GHz, being 52.7 and 1.7 S/m respectively. The radiation patterns of the access point antenna and the antenna of the operator's device are also showed.

### C. Toolkit

The simulations of both models have been solved using the following configuration:

- *Software*: ANSYS Electronics Desktop 2022 R1 HFSS, and the SBR+ ray-tracing solver
  - Maximum wedge angle: 135 °
  - Ray density: 4
  - Maximum number of bounces: 5
- *Hardware*: Windows 10 Pro for Workstations on a Dell Precision 3630 Tower workstation
  - CPU: Intel® Xeon® E-2124, 4 cores @ 3.30 GHz
  - RAM: 32 GB
  - GPU: NVIDIA Quadro RTX 4000 (8 GB GDDR6)

The previous values of ray density and number of bounces have been adjusted to obtain a reasonable computing time. Tests with larger values have also been done for comparison, obtaining similar qualitative results.

## III. RESULTS

In this section the results for WLTB and WLCN are showed.

### A. Wireless Train Backbone

The simulations related to the WLTB are the following ones:

1. The effect of variations on the auxiliary boxes located on the roof of the train car.
2. The effect of a Perfect Electrical Conductor (PEC) tunnel.
3. The effect of changes on the radiation pattern of the antennas.

In these simulations the  $S_{21}$  parameter has been obtained between the two antennas for a bandwidth of 10 MHz centered at 5.9 GHz. In Fig. 3, a ray tracing result example is showed

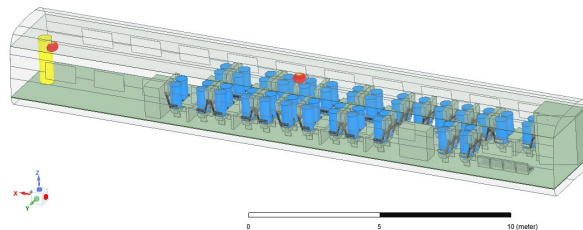


Fig. 2 Train model for WLCN

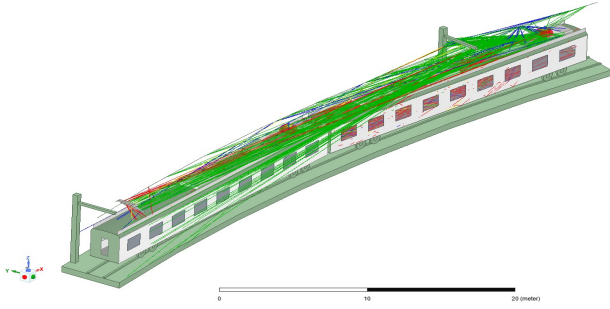


Fig. 3 Ray tracing example in the WLTB simulation

### 1) Auxiliary boxes

#### a) Height

The height of the auxiliary boxes has been changed in the range of 0.05 m – 1.6 m in 5 cm steps (the width of the boxes is 1.6 m, and their lengths are 1 m and 3 m). The results of the mean values in the analysed bandwidth are showed in Fig. 4. Free space values have been included as a reference, drawn as a dotted red line, and standard deviation values have been also included as vertical black lines. It can be observed that slight changes in the height of the auxiliary boxes, has a big effect on the signal reception. There is also a minor decrease in the received signal as the box height increases.

#### b) Distance box-antenna

The distance between the auxiliary boxes and the antenna has been changed in the range of 0.0127 m – 1.033 m in 1.27 cm steps. The results are showed in Fig. 5. As in the previous case, slight changes in the distance have a big effect on the transmission. There is also a minor increase in the received signal when the distance between the antenna and the nearest box wall increases.

#### c) Distance box-roof

The distance between the auxiliary boxes and the roof has been changed in the range of 0 m – 0.6 m in 5 cm steps. The results are showed in Fig. 6. Three zones can be described:

1.  $Distance < 0.25\text{ m}$ : there are multiple reflections between the boxes and the roof.

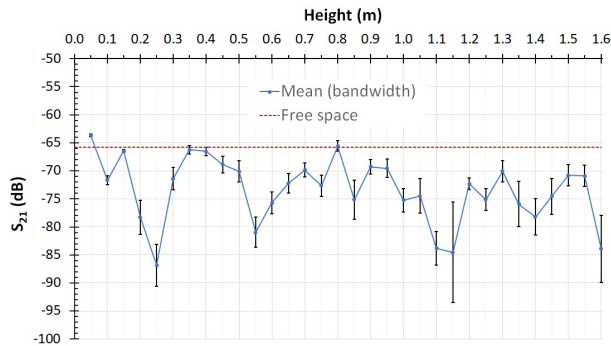


Fig. 4 Effect of the height of the auxiliary boxes

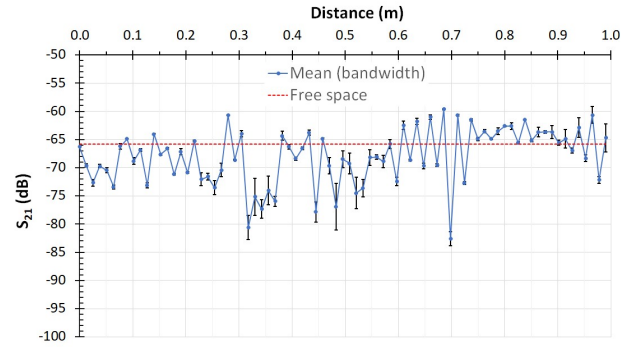


Fig. 5 Effect of the distance between auxiliary boxes and antenna

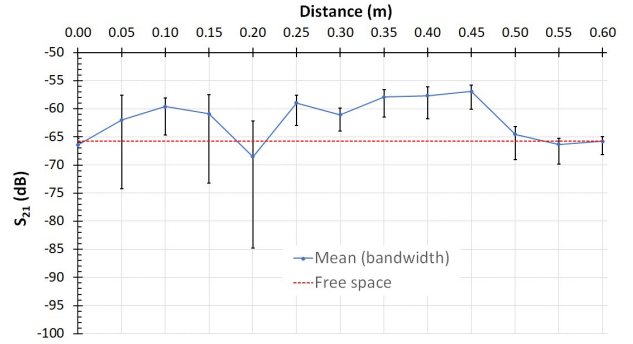


Fig. 6 Effect of the distance between auxiliary box and roof

2.  $0.25\text{ m} < Distance < 0.5\text{ m}$ : there is a waveguide effect, with little variation between frequencies and an increased value
3.  $Distance > 0.5\text{ m}$ : due to the high distance, the boxes have no effect, and the result is equal to free space value

### 2) PEC tunnel

In this section, the external environment is analyzed in terms of a PEC tunnel. This is the worst scenario, in which a continuous highly reflective surface is near the antennas, and the  $S_{21}$  value is increased by 15%. The result is showed in Fig. 7.

### 3) Radiation patterns

The quarter-wave monopole antenna has been replaced by a directive antenna, with a beamwidth of  $40^\circ$  in both

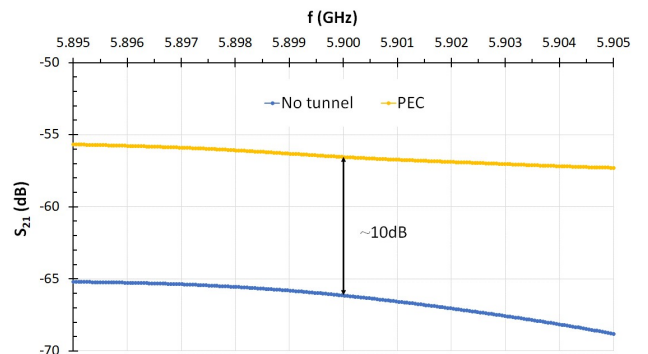


Fig. 7 PEC tunnel effect

vertical and horizontal planes. The radiation pattern of this antenna is showed in Fig. 8.

The azimuth orientation of the directive antenna has been changed in the range of  $0^\circ - 180^\circ$  in  $1^\circ$  steps. The position at  $0^\circ$  is directly facing one auxiliary box,  $90^\circ$  is directly facing the fairing, and  $180^\circ$  is facing the opposite auxiliary box. The results are showed in Fig. 9.

Comparing the results obtained with the directive antenna with the results obtained with the monopole type antenna, a visible gain of the signal is observed, as  $S_{21}$  increases from  $-65$  dB to  $-45$  dB. The highest values are obtained when the antennas are oriented on the train longitudinal axis, directly facing the auxiliary boxes:  $0^\circ$  and  $180^\circ$ .

### B. Wireless Consist Network

The simulations related to the WLCN analyze the variation of the signal along the train car, with the receiver antenna or Access Point (AP) located at the middle of the train car. For this purpose, the  $S_{21}$  parameter has been obtained between the two antennas for a bandwidth of 20 MHz centered at 2.45 GHz. In all the scenarios, the obtained results are not symmetrical, due to the asymmetric nature of the train car configuration (see Fig. 2). In Fig. 10, a ray tracing result example is showed.

#### 1) Sensor Scenario

The position of the sensor starts at 1 m away from the train car wall, moving through the empty part towards the AP, and reaching the end of the train car through the passengers' area. In this scenario, the sensor is located above

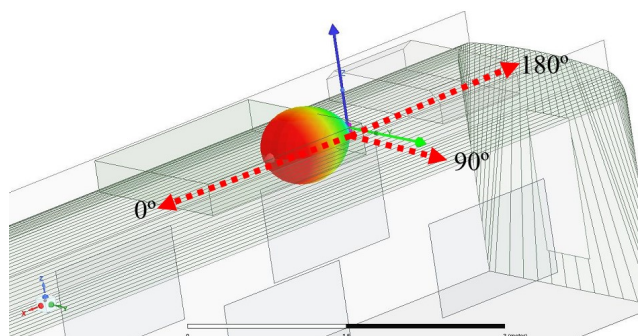


Fig. 8 Radiation pattern of directive antenna

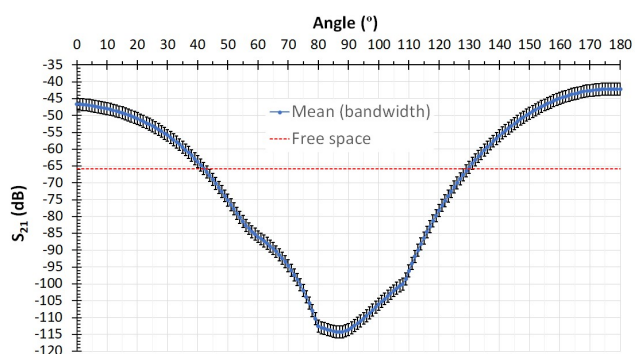


Fig. 9 Effect of the azimuth orientation of the directive antenna

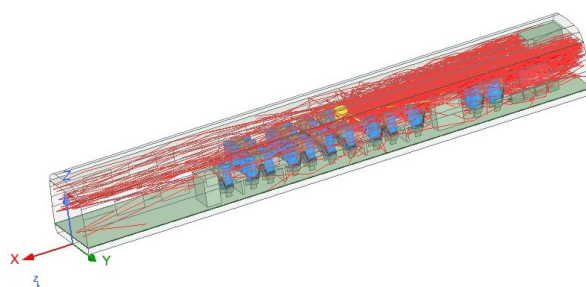


Fig. 10 Ray tracing example in the WLCN simulation

the ceiling of the train car, inside the space between the ceiling and the roof of the train car. In this case the maximum transmission is obtained near the access point, decreasing with the distance, as it can be seen in Fig. 11.

#### 2) Camera Scenario

Similar to the previous scenario, the position of the surveillance camera starts at 1 m away from the train car wall, moving through the empty part towards the AP, and reaching the end of the train car through the passengers' area. In this scenario, the camera is located under the ceiling of the train car, inside the passenger's area. In this case the maximum transmission is also obtained near the access point, decreasing with the distance, as it can be seen in Fig. 12.

Several works have been found in literature which model the path loss at 2.4 GHz in scenarios which are similar to the passenger's area in the WLCN [6]-[8]. In Fig. 13, these

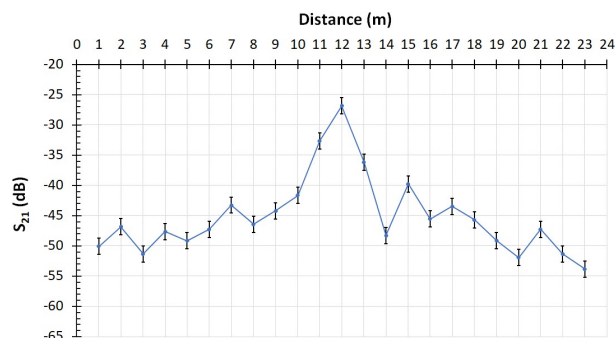


Fig. 11 Sensor position moving along the train car

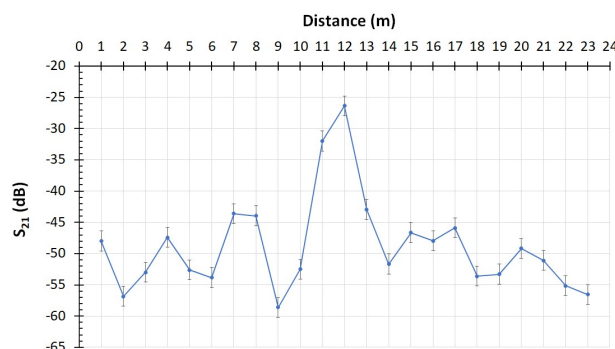


Fig. 12 Camera position moving along the train car



models from literature are compared with the results obtained in the camera scenario. As it can be seen, the logarithmic regression of the WLCN results fits well the ITU-R results for a corridor model.

### 3) Operator Scenario

The position of the operator's mobile device starts at 1 m away from the train car wall, moving through the empty part towards the AP, and reaching the end of the train car through the passengers' area. In this scenario, the antenna of the mobile device is located in front of the operator, at 1.5 m above the floor of the train car, and 0.28 m away from the center of the body. The result is showed in Fig. 14. There are 2 parts, when there is a clear line of sight between the mobile device and the AP, and when the operator's body is hiding the AP.

## IV. CONCLUSIONS AND FUTURE WORK

### A. Wireless Train Backbone

The WLTB propagation is very reflective due to the large number of metallic objects on the train roof and as a consequence the received signal changes with small variations of the environment. Therefore, as directive links are less prone to variations due to the environment, directive antennas are recommended to overcome the problems that arise due to the complex metallic environment.

### B. Wireless Consist Network

The WLCN propagation is also highly reflective, and the following conclusions can be extracted from the obtained results:

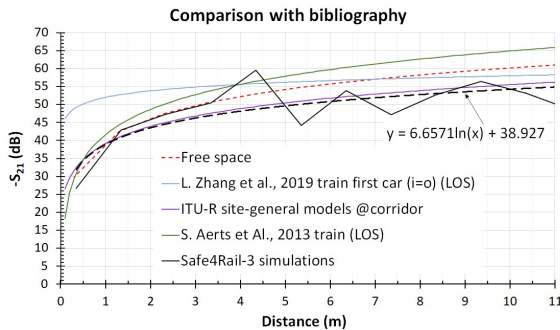


Fig. 13 Comparison with literature

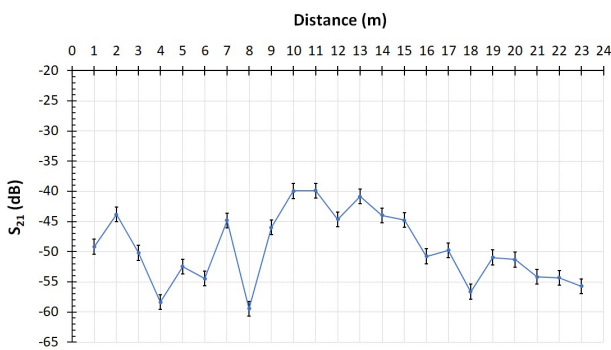


Fig. 14 Operator position moving along the train car

1. In the sensor and camera scenarios, as the device approaches the AP the Line-of-Sight component gets stronger and therefore the effect of the multipath components is reduced, decreasing the variation of  $S_{21}$ .
2. In the operator scenario, the body of the operator has a big effect on the signal when the AP is behind the operator, as the transmission is partially blocked by the body of the operator.

In future activities of the project, these simulation results will be validated in real trains.

## ACKNOWLEDGMENT

This work has received funding from the European Union's Horizon 2020 research and innovation program under grant agreement No: 101015405, Safe4RAIL-3 (<https://safe4rail-3.eu/>).

## DISCLAIMER

The information and views set out in this document are those of the author(s) and do not necessarily reflect the official opinion of Europe's Rail Joint Undertaking (JU). The JU does not guarantee the accuracy of the data included in this article. Neither the JU nor any person acting on the JU's behalf may be held responsible for the use which may be made of the information contained therein.

## REFERENCES

- [1] J. Li, L. Liu, and K. Guan, "Narrow-Band Radio Propagation Prediction Based on a Highly Accurate Three-Dimensional Railway Environment Model," *Wireless Communications and Mobile Computing*, vol. 2022, p. 14, 2022, doi: 10.1155/2022/3341316.
- [2] D. He et al., "Stochastic Channel Modeling for Railway Tunnel Scenarios at 25 GHz," *ETRI Journal*, vol. 40, no. 1, pp. 39-50, 15-02 2018, doi: 10.4218/etrij.2017-0190.
- [3] P. Unterhuber, M. Walter, U.-C. Fiebig, and T. Kumer, "Stochastic Channel Parameters for Train-to-Train Communications," *IEEE Open Journal of Antennas and Propagation*, vol. 2, pp. 778-792, 01-01 2021, doi: 10.1109/ojap.2021.3094672.
- [4] N. Kita et al., "Experimental study of propagation characteristics for wireless communications in high-speed train cars," in *3<sup>rd</sup> European Conference on Antennas and Propagation*, 23-27 March 2009, pp. 897-901.
- [5] J. Elizalde, A. Arriola, M. Alfageme, J. Härri, and I. López, "Characterization of a 5G Wireless Train Backbone via Ray-Tracing," in *16<sup>th</sup> European Conference on Antennas and Propagation (EuCAP)*, 27 March - 1 April 2022, pp. 1-4, doi: 10.23919/EuCAP53622.2022.9769483.
- [6] L. Zhang, J. Moreno, and C. Briso, "Experimental characterisation and modelling of intra-car communications inside high-speed trains," *IET Microwaves, Antennas & Propagation*, vol. 13, no. 8, pp. 1060-1064, 2019, doi: 10.1049/iet-map.2018.6132.
- [7] Propagation data and prediction methods for the planning of indoor radiocommunication systems and radio local area networks in the frequency range 300 MHz to 450 GHz, I. T. Union, 2021. [Online]. Available: [https://www.itu.int/dms\\_pubrec/itu-r/rec/p/R-REC-P.1238-11-202109-I!!PDF-E.pdf](https://www.itu.int/dms_pubrec/itu-r/rec/p/R-REC-P.1238-11-202109-I!!PDF-E.pdf)
- [8] S. Aerts, D. Plets, L. Verloock, E. Tanghe, W. Joseph, and L. Martens, "Empirical path-loss model in train car," in *7<sup>th</sup> European Conference on Antennas and Propagation (EuCAP)*, 8-12 April 2013, pp. 3777-3780.